EAI Endorsed Transactions
on Pervasive Health and Technology
Research Article EAI.EU

Algorithm to detect and calculate the cerebrospinal fluid (CSF) through Magnetic Resonance Imaging (MRI)

Enrique González-Martín[1], Guillermo Sosa-Gómez[2], Omar Rojas[2,*]

[1]Universidad Central Marta Abreu de Las Villas, Santa Clara, Cuba
[2]Universidad Panamericana. Escuela de Ciencias Económicas y Empresariales. Álvaro del Portillo 49, Zapopan, Jalisco, 45010, México

Abstract

INTRODUCTION: An heuristic algorithm for detection and segmentation of cerebrospinal fluid through magnetic resonance imaging is presented. OBJECTIVE: The objective of the method is to calculate the minimum amount of anesthesia to be used in patients at the time of an operation and thus make a decision based on the algorithm. METHODS: The pattern-based CSF segmentation algorithm presented is based on finite cellular automata that takes as input light and dark images obtained from MRI methods. RESULTS: Based on Fieldman's test, results show that the algorithm is as efficient as the decision taken by two different operators regarding the mL of anesthesia to be used in the patient.

Received on 16 October 2019; accepted on 29 October 2019; published on 13 November 2019

Keywords: Cerebrospinal Fluid (CSF), Magnetic Resonance Imaging, Image Registration, region growing

doi:10.4108/eai.13-7-2018.164179

1. Introduction

For the successful performance of a surgery, it is necessary to induce the patient to a condition that does not represent pain or trauma; furthermore, it is necessary that the region to be manipulated cannot be moved by the patient and therefore use of anesthesia is vital [1]. Anesthesia is a controlled medical act in which clinical drugs are used to block the tactile and painful sensitivity of a patient, be it in all or part of his body, and with or without compromise of conscience [2–4]. Anesthesiology is the medical specialty dedicated to the special care of patients during surgical interventions and other processes that may be bothersome or painful (e.g., endoscopy and interventional radiology, amongst others). Anesthesia is also used for treating acute or chronic pain of an extra surgical cause; examples of such uses are analgesia during labor and pain relief in cancer patients [5, 6].

There are several forms of anesthesia placement, all of which vary depending on the region to be paralyzed or the surgical action to be performed. These are divided into: *local anesthesia*, which can be administered as an injection, spray or pruning, only numbs a small and specific part of the body (for example, a foot, a hand or a piece of skin) [7]; *regional anesthesia*, which is injected near a group of nerves, numbing a larger area of the body (for example, below the waist, as in the epidural anesthesia given to women during childbirth), it is often used to help patients feel better during and after surgical interventions [8]; and *general anesthesia*, which aims to ensure that the person remains completely unconscious (or "asleep") during the intervention, without awareness or memories of the intervention. It can be administered intravenously (IV), which requires inserting a needle into a vein, usually in the arm, and leaving it there during the entire procedure, or by in-haling gases or vapors when breathing through a mask or tube. Usually, regional and general anesthesia are combined [9].

Spinal or subarachnoid anesthesia [10], is a type of regional anesthesia conceptually defined as "the administration of a local anesthetic in the subarachnoid space which is capable of causing reversible blockage of

*Corresponding author. Email: orojas@up.edu.mx

nerve and motor nerve conduction." This subarachnoid space is anatomically located between the arachnoid and the pia mater, along with the entire central nervous system, and is occupied by delicate connective tissue trabeculae and intercommunicating channels containing cerebrospinal fluid (CSF), which constitutes a fundamental element of spinal anesthesia [11, 12].

The spinal block [13], belongs to the neuraxial anesthesia group, in which it acts by blocking the painful impulse at the level of the spinal cord, the dura and the arachnoid are perforated, and the anesthetic is introduced into the subarachnoid space. Bier was the one who made the important advance of spinal anesthesia in 1898, when the first planned spinal anesthesia was performed when he administered 3 mL of 0.5% cocaine in a series of 6 patients for surgery of the lower extremities [14]. To achieve spinal block, anesthesia is necessary in specific places of the spine, where the CSF is found.

The lumbosacral CSF volume has a strong effect, inversely proportional to the extent and duration of the spinal block [15]. It should be noted that the same is variable from patient to patient, and its volume may be influenced by some associated factors such as the increase in intra-abdominal pressure (e.g. pregnancy and globular abdomen, amongst others), body mass index (BMI), hyperventilation, structural alterations of the spinal canal such as spinal canal stenosis or the presence of herniated disc. On the other hand, some other factors such as size, age, and sex, cannot be ignored. Several factors allow for a more accurate calculation of the doses of local anesthetic to be used during spinal anesthesia [16], such as: the relative power of the local anesthetic to be used, a number of nodes or spinal nerve roots to block, a minimum effective concentration of local anesthesia.

In this article, we will discuss how to determine the minimum concentration of the local anesthetic, which depends directly on the volume of CSF, that can be determined in a relatively accurate way through magnetic resonance imaging using image-processing techniques such as the registration of images and a *growing region*. CSF lines the spinal cord and brain; it is a plasma ultra-filtrate, colorless, contains glucose, electrolytes, amino acids and other small molecules found in plasma, it has very few proteins and few cells. CSF protects the central nervous system from damage by collision with the surrounding bone structure [17, 18].

The structure of the paper is as follows: Section 2 presents a discussion and revision about the CSF density and volume in terms of each patient and how to measure it. Section 3 presents the method used to segment the CSF using MRI images, based on a Pattern-based CSF segmentation algorithm that uses automatons. Section 4 presents the metrics for the evaluation of segmentations obtained through a computational process. Section 5 presents the evaluation of results and shows how the proposed algorithm emulates a human operator. Finally, Section 6 concludes.

2. Cerebrospinal Fluid's density and volume

It is necessary to know the volume of CSF before giving a patient a local anesthetic, because the minimum effective concentration of the local anesthetic depends on the volume of CSF where it will be deposited. If the same dose is applied, in equal volume and concentration of local anesthetic, to two patients with different volumes of CSF, in the one where the volume is lower, the concentration of the local anesthetic will be higher, and therefore the rostral diffusion of the drug will be greater, reaching a higher level of blockade in relation to the one with a higher volume of CSF .

Spinal anesthesia is a type of regional anesthesia that involves the use of small amounts of local anesthetic injected into the subarachnoid, in order to produce a reversible loss of both sensation and motor functions. Spinal anesthesia provides excellent conditions to perform various types of operations, such as surgical procedures below the navel, obstetric and gynecological procedures of the uterus and perineum, hernias, genitourinary procedures, orthopedic procedures of the hip down, amongst others.

Spinal anesthesia has great advantages [19], compared to general anesthesia, such as: ease of execution, trustworthiness, excellent operating conditions for surgeons, lower costs, gastrointestinal functions return faster, a decrease in pulmonary complications, a decrease in the incidence of thrombus formation and pulmonary embolism

Many factors influence the distribution of spinal anesthesia, some of which have more influence than others. They can be divided into four categories:

1. Characteristics of the local anesthetic
2. Patient characteristics
3. Injection techniques
4. CSF characteristics.

We will focus on the characteristics of the patient and the characteristics of the CSF, because they are related to our research. Patient characteristics include age, weight, intra-abdominal pressure, the anatomical configuration of the spinal cord and the patient's position during and immediately after the injection. Both age and weight are practically insignificant; however, intra-abdominal pressure and the anatomical configuration of the spinal cord have a great influence on the distribution of spinal anesthesia.

As for the characteristics of the CSF, the volume and density influences the weight of the subarachnoid block [20]:

- CSF density: It has an impact on the diffusion of local anesthesia, it is a factor that cannot be controlled by doctors since it depends on each human being's metabolism. It is known that at 37°C, its density is maintained between $1,003 g/cm^3$ to $1,009 g/cm^3$, with an average of $1,006 g/cm^3$
- CSF volume: It is inversely proportional to the weight of the blockage. This is the most important physiological factor. Obese patients have lower CSF volume compared to non-obese patients. The volume of the CSF is influenced by the patient's characteristics (for example abnormal spinal anatomy).

Magnetic resonance imaging (MRI) is a technique in which the patient is placed in a very strong magnetic field and radio frequency waves are passed through the patient's body in short pulses. Each pulse causes a response pulse of radio frequency waves that are emitted by the patient's tissues. The place from which these signals originate and their strength is determined by a computer, which produces a two-dimensional image of a section of the patient. MRIs can be produced in any plane and are produced in the form of a cut, which is no more than a portion of the area from which the image is being taken, see Figure 1. MRI techniques are suitable for obtaining functional and molecular images due to their non-invasive nature and their versatility in the extraction of physiological, biochemical and functional information [21].

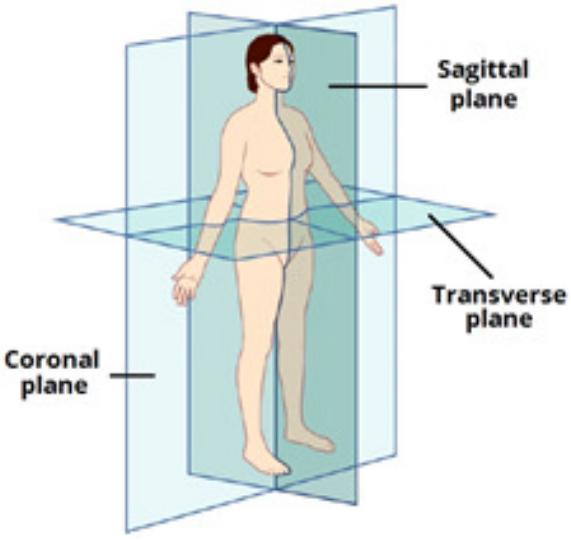

Figure 1. Planes or types of cuts obtained by MRI. Source: Hospital Universitario Arnaldo Milián Castro, Cuba

In addition, these techniques do not introduce radiation to the body as X-rays do, so their continuous use represents minimal risks to human health, so this type of scanner is better for cases when patients need several successive exams in a short space of time. By applying different gradients in the height, width or depth at different times, a complete three-dimensional map of the region of interest can be determined. In addition, these images provide the possibility of obtaining information of intensity, form and even volume of a given region, which turns out to be a good option to calculate the volume of the CSF [22].

In order to calculate the volume of the CSF, it is necessary to obtain, in the best possible way, the portion of the image with which one wishes to work, in this case, the CSF region. Such a process is called *segmentation*, which is nothing more than the process of dividing a digital image into multiple segments (sets of pixels, also known as superpixels). The goal of segmentation is to simplify and/or change a representation of an image into something that has better meaning and is easier to analyze. Image segmentation is typically used to locate objects and neighborhoods (lines, curves, etc.) in images. It is the process of assigning a label to each pixel in an image such that pixels with the same label share certain visual characteristics.

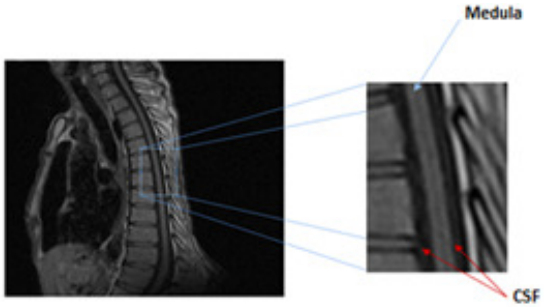

Figure 2. Region of the CSF in MRI type T1. Source: Hospital Universitario Arnaldo Milián Castro, Cuba

Now we explain the types of MRI images used [23]:

- Images of heavy T1 (T1-weighted MRI): Refer to a set of scanning standards that outline differences between various tissues within the body. In the body, scanners with heavy T1 work well to differentiate fat from water, grease appearing lighter and water darker, see Fig. 2.
- Images of heavy T2 (T2-weighted MRI): As in T1 weighing scanners, the fat is differentiated from water, but in this case, the grease appears darker and the water lighter. In the case of the CSF study, it will be clearer in the images of heavy T2. These scanners are particularly good at showing edema, see Fig. 3.

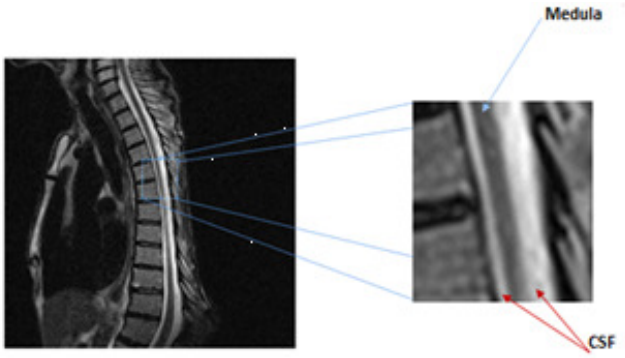

Figure 3. Region of the CSF in MRI type T2. Source: Hospital Universitario Arnaldo Milián Castro, Cuba

As for the registration of images, in many image-processing applications, it is necessary to form a pixel-by-pixel comparison of two images of the same field obtained by different sensors, or of two images of the same field obtained by the same sensor at different times. For this, it is necessary to spatially register the images and correct the translation changes, the rotation differences, scale differences and even the perspective differences of the images [24]. "Image registration is the process of aligning or developing correspondence between the information of several images" [25], see Fig. 4.

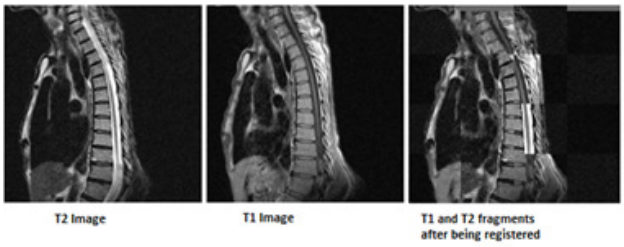

Figure 4. Registration of images. Source: Hospital Universitario Arnaldo Milián Castro, Cuba

Finally, we discuss the connected component, which is a space that cannot be divided into two sets, because each element of that space has some kind of connection with its neighbors; it can also be said that it is a maximal set of nodes, such that there is at least one path connecting both nodes. In the case of images, a connected component can be considered as a maximal set of pixels with similar characteristics (in this case intensity) such that there is at least one path that connects both pixels.

3. Computational method

With the objective of segmenting the CSF, the technique presented in this article takes as input two series of MRI images, the images of type T1 and T2, to produce a 3D image with scalar values assigned to the pixels that allow for the creation of a mask using techniques known in image processing. This algorithm uses a pattern recognition heuristic [26, 27]. It was obtained thanks to the results of research and exchanges with experts in medicine, both anesthesiologists and radiologists. CSF is a liquid of uniform density that covers the spinal cord completely. This information is very important since several observations can be extracted that are taken into account during the development of the algorithm:

Figure 5. Spine. Source: Hospital Universitario Arnaldo Milián Castro, Cuba

1. It covers the entire spinal cord, so in the sagittal plane it will look like two thin layers of the same intensity covering a layer of different intensity, see Fig. 3.

2. The single and continuous CSF, so it extends in the interior and throughout the extension of the spine, see Fig. 5. It is assumed as a related component of uniform density.

3. When an MRI image is observed from the transverse plane, the marrow is seen as a circular area completely covered by the same thin layer of another intensity, this layer that covers the marrow is the CSF. For example, in T1 it should be seen as a clear point covered by a dark layer, see Fig. 6, however, in T2 it looks like a dark spot covered by a layer of clear, see Fig. 7.

4. In the images where the column is shown, the marrow is emphasized, so it is expected that the CSF is a related component of considerable length.

5. In the heavy T1, the pixels of CSF are of low intensity and the fat of high intensity, while in T2 the fat and the water have high intensity.

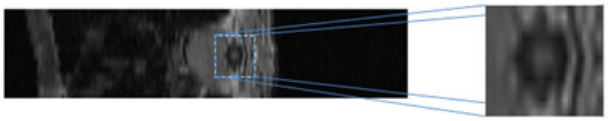

Figure 6. Transverse view of an image T1. Source: Hospital Universitario Arnaldo Milián Castro, Cuba

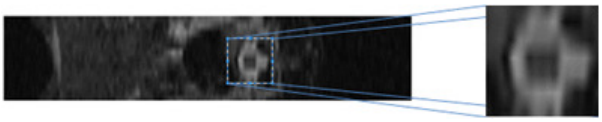

Figure 7. Transverse view of an image T2. Source: Hospital Universitario Arnaldo Milián Castro, Cuba

3.1. Pattern-based CSF segmentation algorithm

The observations made have served as a guide for the proposed algorithm, since the heuristic is based on these to determine the region of the CSF. To obtain seeds (points where to start looking), the algorithm makes a line scan ("scanline"), executing during the scan the finite state automaton $A(X_{ijk})$, see [28]. In Fig. 8 only the entries that change the state to the PLC are shown, the rest are omitted for clarity.

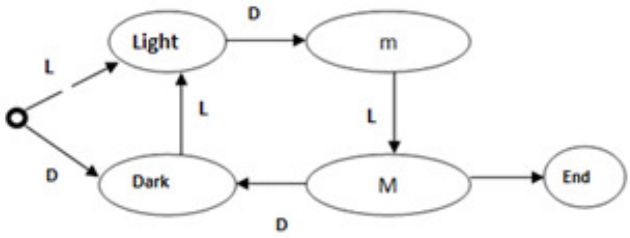

Figure 8. Entries that change the status of the finite state automaton

During the scanline, the automaton is fed with an "L" input whenever a pixel considered "Light" is found (above a certain threshold, i.e. more than 50% of the maximum intensity of the image) and with an input "D" if said pixel is considered "dark" (otherwise):

$$C \ni \left\{X_{ijk} : X_{ijk} > Imax * 0.5\right\}$$

for $O = C'$ and X_{ijk} is the position pixel i, j, k.

Then, if a segment of "scanline" and a given integer value n is found, such that:

$$\left(A\left(X_{ijk}\right) = M\right) \wedge \left(A\left(X_{i,j-n+d,k}\right) = m\right)$$

for all $X_{i,j-n+d,k}$ and $d \in [0, \ldots, n]$. I.e., a segment that complies with the following: a continuous group of dark pixels surrounded by two continuous segments of clear pixels, so the central pixel of the segment is taken as a seed, formally: $X_{i,j-n/2,k}$

This automaton generates multiple false seeds that are discarded. For this, each of the K cross-sections are analyzed, generating two regions $R1_K$ and $R2_K$ with "region-growing":

$$\begin{aligned} R1_K &= g\left(X_{i,j-n/2,K}, \{O\}\right) \\ R2_K &= g\left(X_{i,j-n,K}, \{C\}\right). \end{aligned}$$

From the above, it can be inferred that $R1_K$ is the possible region of the marrow and $R2_K$ the possible CSF area in section K. Unfortunately, this procedure still generates false positives and regions should be discarded $R1_K$ that is not completely contained in their corresponding $R2_k$. In practice this is done for each K-cut, verifying that the minimum dimensions of $R1_K$ are greater than $R2_K$ and its minor maximum dimensions:

$$R1_K^{max} \leq R2_K^{max} \wedge R1_K^{min} \geq R2_K^{min}.$$

R3 is defined as a region containing the CSF throughout the volume of the image. You can take as a seed for a "region-growing" of R3 any pixel in the set of $R2_K$. If R3 contains more than one connected component, the longest one R3' is selected.

As stated above, the whole process is done in T2 so both the fat and the CSF will be linked. To separate them, the image T1 is recorded with T2 and the CSF is obtained as the pixels the intersection between $R3'$ and the set of dark pixels of the image T1:

$$CSF = R3' \cap O_{T1}.$$

3.2. Computational Complexity of the Proposed Algorithm

The search and correction of the CSF region have a computational time equal to the dimensions of the image; i.e., if the image contains $512 \times 512 \times 14$ pixels then: Let N, M, O be the number of pixels in each of the 3 dimensions X, Y, Z, respectively. The computational time of the search and correction of the CSF region will be $O(N * M * O)$. The complexity of image registration depends largely on the library used to perform this complex step, see Alg. 1.

4. Metrics for the evaluation of segmentations obtained through a computational process

Metrics are used as a measurement criterion to know how good the segmentation is. Many times the evaluations are made comparing those obtained in the investigation with existing data and that are assumed

Read Images T1 and T2;
Adjust intensities2;
Register image T1 with T2;
for *each sagittal cut in T2* **do**
  until {the end of the cut is reached,} *Look for the possible CSF area in the sagittal plane (Observation 1)*;
  if *the zone found is completely surrounded (Observation 3)* **then**
    Find Related Component
  end
  Rectify the CSF area of the image T1 with T2;
end
Return the largest connected component;
Calculate the volume of the component
Algorithm 1: Pattern-based CSF Segmentation

as correct. In the case of medical image segmentation, image databases (synthetic or in vivo), segmentation of other techniques, manual segmentation performed by a specialist, etc., are used for comparison. For metallographic images, data obtained from an ISO standard that is known as valid for the materials analyzed can also be used.

The choice of a metric and the validation of an algorithm is not a trivial task. Unfortunately, there are no clear rules as to how to choose an indicator [29]. There are a large number of variables to consider:

1. Define the validation method.
2. The validity of the data assumed as true.
3. Define tolerances at the time of evaluation
4. Are all areas of an ROI really equally important?

Given this, the problem can be complicated. In fact, one segmentation can be good enough for a given purpose and not for another. This is why many of (or all) of the above variables are defined by the users of the application, these being the ones with the final word when deciding. However, it is still necessary to make an estimate of the quality of the segmentation obtained.

To assess the differences between two brain tumor segmentation [30], several similarity coefficients are usually used: Jaccard [31], Hausdorff [32], Dice [33], among others. However, the most common is the Dice similarity coefficient. This coefficient measures the ratio between the intersection region and the average region:

$$DSC\,(A,B) = 2\frac{|A \cap B|}{(|A| + |B|)}.$$

For the CSF, this being a relatively new field, no specific comparison forms were found for this anatomical structure.

Manual segmentation by a specialist is still the reference pattern, in most cases, of medical image segmentation. Unfortunately, it has been seen that it can vary intra and inter-operator. Therefore, in the evaluation of the CSF segmentation algorithm, we tried to demonstrate that the results are alike one or more human operators, verifying that the differences between the algorithm and the human operators do not represent notable differences among themselves. To this end, Friedman's statistical test [34, 35] is used in this comparative study:

$$\chi_F^2 = \frac{12N}{k(k+1)}\left[\sum_j R_j^2 - k(k+1)^2 * 0,25\right],$$

where: $R_j = \frac{1}{N}\sum_i r_i^j$ and r_i^j is the value of the dependent variable j for the i–th data set. N is the number of dependent variables. In this case, the data set i is the value of the Dice metric comparing each of the k segmentations performed by the operators (including the algorithm) against that performed by the i–th operator. Then, r_i^j is replaced by the value of $DSC(i,j)$:

$$R_j = \frac{1}{N}\sum_i DSC(i,j).$$

When interpreting the results, the following is considered: highly significant, a result significantly less than 0.01; significant, a result significantly less than 0.05 and greater than 0.01; mediumly significant, a result less than 0.1 and greater than 0.05; not significant, a result greater than 0.1

5. Evaluation of results

To evaluate the Patter-based CSF segmentation algorithm, we try to confirm that the algorithm behaves like a human operator. Next, the Dice similarity values obtained for the evaluated cases are shown in Table 1.

Cases	Operator 1 vs Operator 2 (%)	Operator 1 vs Algorithm	Operator 2 vs Algorithm
1	72,06	68,08	69,07
2	72,03	70,00	71,08
3	77,05	75,08	73,05
4	70,09	72,05	69,00
5	76,08	72,05	68,02
6	70,08	69,08	70,04

Table 1. Dice similarity values obtained by the algorithm for the evaluated cases

With an asymptotic significance between 0.05 and less than 0.1, the test shows that there are no significant differences, see Table 2.

N	6
χ^2	6.333
gl	2
asymptotic significance	0.042

Table 2. Friedman's statistical test results

Finally, the CSF volumes obtained by segmentation are compared, as shown in Table 3.

Case	Operator 1	Operator 2	Algorithm
1	10,395 mL	10,305 mL	7,663 mL
2	9,245 mL	13,769 mL	16,506 mL
3	15,656 mL	19,564 mL	20,489 mL
4	11,789 mL	15,369 mL	12,467 mL
5	11,789 mL	15,369 mL	12,467 mL
6	18,276 mL	17,438 mL	16,713 mL

Table 3. Volumes of CSF obtained by segmentation.

In this section, only the results are reported, since it was not possible to find another CSF segmentation algorithm with which to compare the efficiency.

6. Conclusions

Despite not being multiple test cases or another similar algorithm with which to compare the proposed algorithm, it has been possible to perform a comparison of the behavior of said algorithm with respect to the response that a human being would provide, and it could be demonstrated that there are no differences significant between the algorithm and a human being. The algorithm can be considered as the first step in order to determine the volume of the CSF efficiently and semi automatically. As a future line of research, more experiments are recommended in order to fine tune the algorithm and pursue the implementation of an automatic decision model, built as an expert system.

References

[1] Barash, P.G., Cullen, B.F., Stoelting, R.K., Cahalan, M.K. and Stock, M.C. (2009) *Clinical Anesthesia* (Philadelphia, PA: Lippincott Williams & Wilkins).

[2] Alkire, M.T., Hudetz, A.G. and Tononi, G. (2008) Consciousness and anesthesia. *Science* **322**(5903): 876–880.

[3] Bonhomme, V., Staquet, C., Montupil, J., Defresne, A., Kirsch, M., Martial, C., Vanhaudenhuyse, A. *et al.* (2019) General anesthesia: A probe to explore consciousness. *Frontiers in Systems Neuroscience* **13**: 36. doi:10.3389/fnsys.2019.00036, URL https://www.frontiersin.org/article/10.3389/fnsys.2019.00036.

[4] Suzuki, M. and Larkum, M.E. (2020) General anesthesia decouples cortical pyramidal neurons. *Cell* **180**(4): 666 – 676.e13. doi:https://doi.org/10.1016/j.cell.2020.01.024, URL http://www.sciencedirect.com/science/article/pii/S0092867420301057.

[5] Hasanzadeh-kiabi, F. and Negahdari, B. (2019) Applications of drug anesthesia in control chronic pain. *Journal of Investigative Surgery* **32**(3): 232–237. doi:10.1080/08941939.2017.1397230, URL https://doi.org/10.1080/08941939.2017.1397230. PMID: 29256718, https://doi.org/10.1080/08941939.2017.1397230.

[6] Rudin, D. (2019) Continuous regional anesthesia or a single shot technique for acute postoperative pain treatment? *Anaesthesia, Pain & Intensive Care* : 297–300.

[7] Wright, J., MacNeill, A.L. and Mayich, D.J. (2019) A prospective comparison of wide-awake local anesthesia and general anesthesia for forefoot surgery. *Foot and Ankle Surgery* **25**(2): 211–214.

[8] Ardon, A.E., Prasad, A., McClain, R.L., Melton, M.S., Nielsen, K.C. and Greengrass, R. (2019) Regional anesthesia for ambulatory anesthesiologists. *Anesthesiology Clinics* **37**(2): 265–287. doi:10.1016/j.anclin.2019.01.005, URL https://doi.org/10.1016/j.anclin.2019.01.005.

[9] Types of Anesthesia (for Teens). URL https://kidshealth.org/en/teens/anesthesia-types.html.

[10] Biebuyck, J.F. and Fink, B.R. (1989) Mechanisms of differential axial blockade in epidural and subarachnoid anesthesia. *Anesthesiology: The Journal of the American Society of Anesthesiologists* **70**(5): 851–858.

[11] Miller, R.D. [ed.] (2010) *Miller's Anesthesia* (Philadelphia, PA: Churchill Livingstone Elsevier).

[12] Longnecker, D., Mackey, S.C., Newman, M.F., Sandberg, W.S. and Zapol, W.M. (2018) *Anesthesiology* (McGraw Hill), 3rd ed.

[13] Moore, D.C. and Bridenbaugh, L.D. (1966) Spinal (subarachnoid) block: a review of 11,574 cases. *Jama* **195**(11): 907–912.

[14] Colbern, E.C. (1970) The bier block for intravenous regional anesthesia: technic and literature review. *Anesthesia & Analgesia* **49**(6): 935–940.

[15] Fink, B.R. (1992) Toward the mathematization of spinal anesthesia. *Regional Anesthesia: The Journal of Neural Blockade in Obstetrics, Surgery, & Pain Control* **17**(5): 263–273.

[16] Ankcorn, C. and Casey, W. (1993) Spinal anaesthesia - a practical guide. *Update in Anaesthesia* **3**: 2–15.

[17] McPherson, R.A. and Pincus, M.R. (2017) *Henry's Clinical Diagnosis and Management by Laboratory Methods* (Elsevier Health Sciences).

[18] Brown, P., Davies, S., Speake, T. and Millar, I. (2004) Molecular mechanisms of cerebrospinal fluid production. *Neuroscience* **129**(4): 955 – 968. doi:https://doi.org/10.1016/j.neuroscience.2004.07.003, URL http://www.sciencedirect.com/science/article/pii/S0306452204005640. Brain Water Homeostasis.

[19] Felsby, S. and Juelsgaard, P. (1995) Combined spinal and epidural anesthesia. *Anesthesia & Analgesia* **80**(4): 821–826.

[20] Van Zundert, A., Grouls, R., Korsten, H. and Lambert, D. (1996) Spinal anesthesia: volume or concentration—what matters? *Regional Anesthesia: The Journal of Neural Blockade in Obstetrics, Surgery, & Pain Control* **21**(2): 112–118.

[21] Prasad, P.V. [ed.] (2006) *Magnetic Resonance Imaging: Methods and Biologic Applications* (Totowa, NJ: Humana Press).

[22] Allison, W. (2006) *Fundamental Physics for Probing and Imaging* (Oxford: Oxford University Press).

[23] Belkic, K. (2004) *Molecular Imaging through Magnetic Resonance for Clinical Oncology* (Cambridge, Great Britain: Cambridge International Science Publishing).

[24] Pratt, W.K. (2014) *Introduction to Digital Image Processing* (Boca Raton, FL: CRC press).

[25] Schroeder, W., Ng, L. and Cates, J. (2005) The itk software guide second edition updated for itk version 2.4. *FEBS Lett* **525**: 53–8.

[26] Kim, J. and Pearl, J. (1983) A computational model for causal and diagnostic reasoning in inference systems. In *International Joint Conference on Artificial Intelligence*: 0–0.

[27] Gigerenzer, G. and Todd, P.M. (1999) *Simple Heuristics that Make Us Smart* (Oxford University Press).

[28] Mainzer, K. and Chua, L. (2011) *The universe as automaton: From simplicity and symmetry to complexity*, **1** (Springer Science & Business Media).

[29] Ibanez, L., Schroeder, W., Ng, L. and Cates, J. (2005), The itk software guide: updated for itk version 2.4.

[30] Cichosz, S.L., Vangsgaard, S., Jørgensen, A.S., Kannik, K.E., Steffensen, E. and Eskildsen, S.F. (2010) Brain tumor segmentation from mri: a comparative study. In *IADIS Multi Conference on Computer Science and Information Systems: Computer Graphics, Visualization, Computer Vison and Image Processing, Web Virtual Reality and Three-dimensional Worlds, Visual Communication* (International Association for Development, IADIS): 401–406.

[31] Jaccard, P. (1912) The distribution of the flora in the alpine zone. 1. *New Phytologist* **11**(2): 37–50.

[32] Öberg, P. (2013) Segmentation of the cardiovascular tree in 4d from pc-mri images. *LUTFMA-3244-2013* .

[33] Dice, L.R. (1945) Measures of the amount of ecologic association between species. *Ecology* **26**(3): 297–302.

[34] Friedman, M. (1937) The use of ranks to avoid the assumption of normality implicit in the analysis of variance. *Journal of the American Statistical Association* **32**(200): 675–701.

[35] Demšar, J. (2006) Statistical comparisons of classifiers over multiple data sets. *Journal of Machine Learning Research* **7**(Jan): 1–30.